A&A 374, 957–967 (2001)
DOI: 10.1051/0004-6361:20010645

Astronomy & Astrophysics

Physical parameters of λ Bootis stars⋆

E. Solano[1], E. Paunzen[2], O. I. Pintado[3,⋆⋆], and J. Varela[4]

[1] Laboratorio de Astrofísica Espacial y Física Fundamental (LAEFF), Apartado de Correos 50727, 28080 Madrid, Spain
e-mail: esm@vilspa.esa.es
[2] Institut für Astronomie der Universität Wien, Türkenschanzstr. 17, 1180 Wien, Austria
e-mail: Ernst.Paunzen@univie.ac.at
[3] Departamento de Física, Facultad de Ciencias Exactas y Tecnología, Universidad Nacional de Tucumán, Argentina – Consejo Nacional de Investigaciones Científicas y Técnicas de la República Argentina
e-mail: opintado@tucbbs.com.ar
[4] IMAFF, Consejo Superior de Investigaciones Científicas, c/ Serrano 113, 28006 Madrid, Spain
e-mail: jesusv@imaff.cfmac.csic.es

Received 7 December 2000 / Accepted 26 April 2001

Abstract. This is the first of two papers whose main goal is to update and improve the information available on the physical properties of the λ Bootis stars. The determination of the stellar parameters is of fundamental importance to shed light into the different theories proposed to explain the λ Bootis phenomenon. With this aim, projected rotational velocities, effective temperatures, surface gravities and chemical abundances of a sample of suspected λ Bootis stars have been calculated. Five objects showing composite spectra typical of binary systems were found in our analysis. The abundance distribution of the program stars does not resemble the chemical composition of the class prototype, λ Boo, which poses some concerns regarding the idea of a well-defined, chemically homogeneous group of stars. A possible relation between rotational velocities and the λ Bootis phenomenon has been found. This result would be in agreement with the accretion scenario proposed by Turcotte & Charbonneau (1993).

Key words. stars: chemically peculiar – stars: abundances

1. Introduction

λ Bootis stars have been defined as late B to mid F, metal-weak, Population I objects (Paunzen 2000). The nature and evolutionary state of these stars is still a matter of debate and different hypothesis can be found in the literature.

1.1. Very young stars which have not reached the Main Sequence

This theory, suggested by Venn & Lambert (1990), supports the idea of a star surrounded by a shell of gas and dust, the volatile elements remaining in the gaseous phase while the refractory elements, with a higher condensation temperature, are locked in the dust grains. The depleted gas is accreted by the star whereas the dust grains are swept away from the shell due to radiation pressure. Waters et al. (1992) and Andrievsky & Paunzen (2000) have proposed scenarios where the dust–gas decoupling is always present in regions where the temperature drops to a value less than the condensation temperature of the heavy elements.

Observational results supporting the accretion theory are the high [C/Si] and [O/Si] abundance ratios found in some λ Bootis stars which can be used as indicators of gas-dust separation (Paunzen et al. 1999a): carbon and oxygen have low condensation temperatures and tends to remain in the gas phase of the interstellar medium. Silicon, on the other side, has a high condensation temperature representing the elements locked up in the grains. Any preferential accretion of gas will lead to a [C/Si] or [O/Si] larger than solar. The correlation with Si of other elements of high condensation temperature also fits nicely with the accretion scenario (Stürenburg 1993). Charbonneau (1991) combined the accretion hypothesis with the diffusion theory concluding that, with an accretion rate of the order of 10^{-13} $M_\odot$ yr^{-1}, many peculiar characteristics of the λ Bootis stars (including their restriction to the

Send offprint requests to: E. Solano,
e-mail: esm@vilspa.esa.es

⋆ Figure 3 is only available in electronic form at http://www.edpsciences.org

⋆⋆ Visiting Astronomer at CASLEO. Complejo Astronómico El Leoncito (CASLEO) is operated under agreement between the Consejo Nacional de Investigaciones Científicas y Técnicas de la República Argentina and the National Universities of La Plata, Córdoba y San Juan.

above-mentioned spectral types) are reproduced quite naturally. Turcotte & Charbonneau (1993) investigated the effect of mixing through meridional circulation, concluding that the abundance anomalies would disappear in 10^6 years, so all of the λ Bootis stars should be essentially young objects on or just arriving to the ZAMS. The scarcity of λ Bootis will be also explained by the strict requirements for the accretion rate. The fact that all λ Bootis stars are young objects is further strengthened by the lack of λ Bootis stars in open clusters older than 10^7 years (Gray & Corbally 1988) and the discovery of λ Bootis stars in the young Orion OB1 association and NGC 2264 (Paunzen & Gray 1997).

A critical point in the accretion scenario is the necessary existence of gas and dust shells around λ Bootis stars. Some λ Bootis stars show clear indications of both gas (circumstellar lines) and dust (IR excess) shells (Holweger & Rentzsch-Holm 1995; Holweger et al. 1999). However, the fact that some λ Bootis stars do not show evidence of shells does not necessary rule out this hypothesis. King (1994) concluded that the amount of depleted gas required to cause underabundances in λ Bootis stars is small enough that any circumstellar dust associated with this gas is not necessarily detectable in the IR or submillimetre regions.

1.2. Stars at the end of their Main Sequence lifetime

Michaud & Charland (1986) investigated the effect on abundances in stellar atmospheres of the diffusion mechanism operating in the presence of mass loss. They found that, after about 10^8–10^9 years, mass-loss rates of only 10^{-13} $M_\odot$ yr^{-1} can reduce the extreme overabundances predicted by diffusion theory for the Am stars to underabundances of many elements, the degree of underabundance of an element being a function of both gravity and time. According to this, λ Bootis stars would be rather old and at the end of their Main Sequence.

There are, however, some points that cannot be explained with theory. One is the moderate underabundances predicted (only a factor of five less solar), very far from the strong underabundances found by Venn & Lambert (1990) in the three classical λ Bootis stars (λ Boo, π^1 Ori and 29 Cyg). Also it is difficult to understand how diffusion could operate in the presence of the meridional circulation which would likely be generated by rapid rotation. Turcotte & Charbonneau (1993) showed that even an equatorial rotational velocity of 50 kms^{-1} suppresses the appearance, at any epoch of Main Sequence evolution, of the characteristic λ Bootis abundance pattern.

1.3. Spectroscopic binary theory

Faraggiana & Bonifacio (1999) proposed this alternative to explain the underabundances of, at least, some λ Bootis stars. The composite spectra of a binary system with disentangled components not very dissimilar produces a veiling effect with apparent underabundances. The authors pointed out that the lack of a uniform pattern in the chemical composition of the λ Bootis stars can be easily reconciled with the binary hypothesis. Moreover, they claimed that the hypothesis of all λ Bootis stars being very young objects in the late phase of their PMS evolution is highly improbable on the basis of the rapid evolution and the number of bright λ Bootis candidates which would imply that the star formation process is still very active in the solar neighborhood, leading to an unexpected large number of Main Sequence B stars in a similar volume.

1.4. Contact binary theory

Andrievsky (1997) proposed a complementary scenario in which λ Bootis stars would be the result of the coalescence of contact binaries of W UMa type. The system would be formed by two main-sequence components of approximately equal spectral types. This scenario would lead to an age for λ Bootis stars of 1 Gyr explaining the rather evolved nature of some λ Bootis stars and the origin of the material around them.

A class definition of the λ Bootis group is essential on one hand to distinguish these stars from other groups of stars populating the same region of the HR diagram and, on the other hand, to shed light into the nature of the λ Bootis phenomenon. Ideally, a stellar class should be formed by a homogeneous sample of stars showing common properties originated by the same astrophysical processes. Historically, this has not been the case for the λ Bootis group since the use in the past of classification criteria not unique to the group (weakness of the Mg II 4481 Å line, presence of spectral features at 1600 Å and 3040 Å, IR excess, ...) has led to the inclusion of spurious members (horizontal branch stars, Ap stars, shell stars, He-weak stars, ...). Although the problem of the class definition can be efficiently alleviated making use of unambiguous criteria defined in the ultraviolet range (Solano & Paunzen 1998, 1999), the chemical composition-based definition of the class makes it necessary to perform an accurate determination of the stellar parameters for the final decision on the membership of a potential candidate to the λ Bootis group. The observed sample was selected from the list of suspected λ Bootis stars given in Paunzen (2000). HD 68758 and HD 184190 were also included as possible members of the class.

2. Observations and data reduction

The observations were performed in May 1998 at the Complejo Astronómico el Leoncito (CASLEO) using the 2.15-m telescope equipped with a REOSC echelle spectrograph[1] and a Tek-1024 CCD. A grating with

[1] On loan from the Institute Astrophysique de Liège, Belgium.

1200 lines mm^{-1} was used as a cross disperser. A resolving power of 26 000 was achieved. Two wavelength ranges were observed (3830–4570 Å; 4520–5230 Å).

The spectra were reduced using the context echelle of the MIDAS reduction package. A typical session of echelle reduction comprises the following steps: bias subtraction, spatial positioning of the spectral orders, flatfield correction (several master flatfield exposures were taken every night), background subtraction, order extraction and wavelength calibration. The wavelength calibration of the stellar spectra was done with thorium-argon comparison spectra. Polynomial calibrations of wavelength as a function of pixel number were calculated for every night. The lower sensitivity at the edges of the orders typical of echelle spectra (ripple effect) was corrected by using Procyon as standard star. A blaze function was derived for each order.

The reliability of the measured equivalent widths depends to a great extent on the accuracy of the continuum placement: an improper placement of the continuum level will lead to systematic errors which can misrepresent the data. Most λ Bootis stars are characterized as having broad and often shallow absorption line profiles. In this case, the continuum placement cannot be set by simply connecting the highest points in the observed spectrum, which would produce an underestimation of the equivalent widths. We solved this problem by defining the "true" continuum level as that of a synthetic spectrum of physical parameters ($T_{\rm eff}$, log g, [M/H], $v \sin i$) similar to those of the observed object. As a first approach, effective temperatures and surface gravities were derived using Moon & Dworetsky (1985). Rotational velocities were estimated using the method described in Sect. 3 where a pseudo-continuum was defined by connecting the highest points in the line profile: the small influence of the continuum level on the method used to calculate rotational velocities permits this approximation. Also, a value of [M/H] $= -1.0$ was used for all the stars, which is justified by the results from our detailed abundance analysis. The normalized spectra were then derived by dividing the extracted spectra by this continuum level. Line identification was performed with the help of Moore et al. (1966).

To have an estimation of the measurements errors in equivalent widths, the standard star Procyon (α CMi, HR 2943) was observed and the spectra compared to the spectrum of the Atlas of Procyon (Griffin & Griffin 1979). It can be seen in Table 1 how the equivalent widths measured in the observed spectra are only slightly larger than those measured in the Atlas. We also compared the equivalent widths of spectral lines present in the overlapping region between spectral orders finding no systematic trend. The list of observed objects is given in Table 2.

2.1. Binarity among the observed stars

Five targets of our sample show a composite spectra and no attempt to derive their abundance pattern was done (Fig. 1). All of them are identified as members of binary systems:

Table 1. Comparison between the equivalent widths measured in the observed spectra of Procyon and in the Atlas (Griffin & Griffin 1979). The relative error is defined as $(EW(\text{observed}) - EW(\text{atlas}))/EW(\text{atlas})$.

Observing date	Relative error	Number of lines
08/05/1998	0.05 ± 0.14	12
09/05/1998	0.06 ± 0.08	9
10/05/1998	0.02 ± 0.12	11
11/05/1998	0.04 ± 0.15	11
12/05/1998	0.02 ± 0.06	20
13/05/1998	0.07 ± 0.11	17

- **HD 111786:** Two different hypothesis have been formulated for this star: Holweger & Rentzsch-Holm (1995) recognized a variable narrow absorption in the core of the Ca II K line interpreted as sign of gas dynamic in an accretion disc whereas Faraggiana et al. (1997) proposed a double-line spectroscopic binary system in which the narrow features shown in the spectrum belong to a slow-rotating early F-type star;
- **HD 141851:** Catalogued as visual binary (Faraggiana & Bonifacio 1999). The small separation of the pairs ($0.1''$) makes that ground-based spectra will always be the combined spectrum;
- **HD 148638:** This object is identified in HIPPARCOS as double system with the two components of similar magnitude and a maximum separation of $21.9''$;
- **HD 174005:** Catalogued as spectroscopic binary (Paunzen 2000), the maximum separation between components is $37.9''$;
- **HD 177120:** Catalogued as a visual multiple system (Abt 1985), the separation between the primary and secondary being of $8''$ (Faraggiana & Bonifacio 1999).

3. Rotational velocities

Different methods can be found in the literature to calculate rotational velocities. In this work we have used the technique based on the Fourier transform proposed by Gray (1992) which has shown to give superior results than those based on the convolution of a non-rotating standard star of similar spectral type with a rotational function or on the identification of a particular parameter of the spectral lines (e.g. $FWHM$). Whereas these two latter methods require one to build up a calibration of rotational velocities, Gray's method provides a direct and independent measurement of $v \sin i$. In short, the method relies on the relation between $v \sin i$ and the frequencies where the Fourier transform of the rotational profile reaches a relative minimum. Instrumental broadening may add relative minima in the Fourier transform but at higher frequencies than those used to calculate the rotational velocity. Projected rotational velocities for our sample of stars are given in Table 2.

Table 2. Target list. Spectral types (excluding HD 184190 for which SIMBAD was used) and visual magnitudes are taken from Paunzen (2000) and SIMBAD, respectively. Surface gravities derived from HIPPARCOS parallaxes are labeled with (∗). Adopted values (in boldface) are the average of Balmer lines and Moon & Dworetsky (1985) ($T_{\rm eff}$), HIPPARCOS and Moon & Dworetsky (1985) (log g) and the weighted mean of the different measurements ($v \sin i$). Steps of 50 K and 0.1 dex have been assumed.

Identification	Spectral. type	V mag.	Region (Å)	$T_{\rm eff}$ This work /Other sources	log g This work /Other sources	$v \sin i$ This work /Other sources
HD 68758	A1IVp	6.52	3830-4570			291 ± 21 (2)
			3830-4570	8100(H_γ),8187(H_δ)		299 ± 23 (3)
			3830-4570	8050(H_δ)		305 ± 25 (6)
			3830-4570	8066(H_δ)		297 ± 41 (3)
			4520-5230			285 (1)
				/8300(4)	/3.7(∗),3.65(4)	
				8150	**3.7**	**299**
HD 75654	hF0mA5V	6.38	3830-4570	7256(H_γ),7214(H_δ)		45 ± 4 (16)
			4520-5230			43 ± 5 (13)
				/7275(4),7200(10)	/3.85(∗),3.8(4),3.8(10)	/45(10)
				7250	**3.8**	**44**
HD 81290	kA5hF3mA5V	8.89	3830-4570	6775(H_γ),6862(H_δ)		53 ± 6 (10)
			3830-4570			57 ± 8 (7)
			4520-5230	6800(H_β)		56 ± 8 (16)
			4520-5230	6750(H_β)		57 ± 8 (18)
				/6750(4),6760(6)	/3.5(4)	
				6800	**3.5**	**56**
HD 83041	kA2hF2mA2V	8.80	3830-4570			105 ± 15 (7)
			3830-4570			106 ± 17 (4)
			3830-4570	6800(H_δ)		121 ± 33 (4)
			4520-5230	7050(H_β)		77 ± 10 (9)
			4520-5230	6975(H_β)		83 ± 14 (6)
			4520-5230	6843(H_β)		78 ± 10 (6)
				/6850(4),6900(6)	/3.6(4),3.3(6)	
				6900	**3.6**	**95**
HD 107233	kA1hF0mA1Va A1V	7.37	3830-4570	7000(H_γ),6900(H_δ)		112 ± 11 (24)
			3830-4570	6900(H_γ),6950(H_δ)		110 ± 12 (17)
				/7225(4),7244(5),7200(2)	/4.2(∗), 4.05(4), 4.1(2)	
				7000	**4.1**	**111**
HD 109738	kA1hA9mA1V	8.29	3830-4570	7437(H_γ),7350(H_δ)		185 ± 18 (10)
			3830-4570	7425(H_δ)		164 ± 5 (3)
				7500(H_β)		170 ± 14 (2)
				7500(H_β)		167 ± 12 (6)
				/7575(4),7603(6)	/3.9(4),3.8(6)	
				7450	**3.9**	**166**
111005	hF0mA3V	7.97	3830-4570	7250(H_γ),7330(H_δ)		140 ± 15 (12)
			3830-4570	7415(H_γ),7380(H_δ)		131 ± 12 (10)
			3830-4570	7525(H_γ),7375(H_δ)		136 ± 12 (8)
			4520-5230	7500(H_β)		143 ± 13 (5)
			4520-5230	7500(H_β)		142 ± 11 (6)
					/ 3.8(∗)	
				7400	**3.8**	**138**
HD 142703	kA1hF0mA1Va	6.13	3830-4570	7172(H_γ),7000(H_δ)		120 ± 13 (16)
			4520-5230			110 ± 20 (12)
				/7200(4), 7400(2),7294(6)	/4.1(∗),4.1(2),3.95(4)	/100(10),95(12)
				7100	**4.0**	**117**
HD 142994	A3Va	7.18	3830-4570	6900(H_γ),6962(H_δ)		202 ± 14 (10)
			3830-4570	7035(H_γ),6803(H_δ)		212 ± 14 (9)
			4520-5230			204 ± 10 (9)
			4520-5230			207 ± 17 (10)
				/7079(1),7244(2),7000(4)	/3.5(1,2,3),3.4(4)	/220(1),195(3)
				6950	**3.4**	**206**

Table 2. continued.

Identification	Spectral. type	V mag.	Region (Å)	$T_{\rm eff}$ This work /Other sources	log g This work /Other sources	$v \sin i$ This work /Other sources
HD 156954	hF1mA5V	7.69	3830-4570	6775(H_γ),7112(H_δ)		47 ± 7 (20)
			3830-4570	7000(H_γ),		53 ± 9 (21)
			4520-5230	6937(H_β)		56 ± 9 (32)
				/7050(4),7079(6)	/4.2(∗),4.0(4)	
				7000	**4.1**	**51**
HD 168740	hA7mA2V	6.13	3830-4570	7875(H_γ),7650(H_δ)		168 ± 16 (12)
			4520-5230	7575(H_β)		158 ± 14 (10)
				/7650(4),7700(10)	/4.15(∗), 3.9(4,12)	/147 (10)
				7700	**4.0**	**162**
HD 184190	A8	9.74	4520-5230	7200(H_β)		19 ± 3 (55)
				7250(4)	4.0(4)	
				7250	**4.0**	**19**
HD 193281	hA3mA2Vb	6.30	3830-4570	8000(H_γ),8000(H_δ)		101 ± 7 (5)
			4520-5230			103 ± 9 (7)
			4530-5230			104 ± 5 (6)
				/8100(4), 8100(10), 8080(13)	/3.5(4),3.6(10),3.6(13)	/95(10), 83(13)
				8050 K	**3.5**	**103**
HD 204041	A1Vb	6.46	3830-4570	7857(H_γ),8041(H_δ)		68 ± 5 (8)
			3830-4570	7950(H_γ),8118(H_δ)		69 ± 7 (10)
			4520-5230	7950(H_δ)		70 ± 5 (7)
				/8100(4),8128(6),8100(7)	/4.0(∗),3.95(4),4.03(7)	/65(7),68(8),70(11)
				8000	**4.0**	**69**
HD 210111	kA2hA7mA2Vas		3830-4570			57 ± 6 (10)
			3830-4570			54 ± 9 (9)
			4520-5230	7415(H_β)		60 ± 11 (8)
				/7762(2),7603(5),7450(4)	/3.9(∗),3.9(2),3.8(4),3.75(8)	/55(8),60(11)
				7450	**3.8**	**57**

References: (1) Paunzen et al. (1998a); (2) Iliev & Barzova (1995); (3) Bohlender et al. (1999); (4) Moon & Dworetsky (1985); (5) Paunzen (1997); (6) Paunzen et al. (1998b); (7) Stürenburg (1993); (8) Holweger & Rentzsch-Holm (1995); (9) North et al. (1994); (10) Paunzen et al. (1999a); (11) Gray & Corbally (1993); (12) Faraggiana & Bonifacio (1999); (13) Holweger et al. (1999).

4. Effective temperature

It is well established that the Balmer lines are good temperature indicators for $T_{\rm eff} \leq 8000$–8250 K because of their small gravity and metallicity dependence (Solano & Fernley 1997). As the spectral orders are not wide enough to fully embrace the wings of the observed Balmer lines (H_δ, H_γ, H_β), an alternative method based on the variations in intensity at two different wavelengths was used instead. These wavelengths, free of contamination of metallic lines, were selected in such a way that they lie in the region of the Balmer line profile where the dependency with temperature is maximum. Prior to this, the observed Balmer lines were shifted to the laboratory values to correct for radial velocity displacements. Effective temperatures were then calculated by comparing the observed intensity ratio with the intensity ratio measured in a grid of synthetic Balmer profiles previously convolved with the corresponding rotational and instrumental profiles.

Balmer lines are known to be very sensitive to convection as it can alter the temperature structure where the lines are formed. In this work, the turbulent convection model developed by Canuto et al. (1996) and implemented in the ATLAS9 code by Kupka (1999) has been used. This convection model has been found to reproduce adequately the temperature of standard stars whereas the standard mixing-length theory models with overshooting, originally implemented in ATLAS9, are clearly discrepant (Gardiner et al. 1999; Smalley & Kupka 1997). The effective temperatures are given in Table 2. An error of $\Delta T_{\rm eff} = \pm 200$ K has been assumed.

Some concern may also exist in the use of Balmer lines as temperature indicators due to the existence of peculiar Balmer profiles (weak, narrow core typical of late A-type dwarfs but with strong wings proper to early A-type dwarfs) in some λ Bootis stars (Gray 1988). Based on this criterion, λ Bootis stars have been traditionally classified in two groups: normal hydrogen-lines (NHL) and peculiar hydrogen-line profiles (PHL). Iliev & Barzova (1993) suggested that PHL profiles could be fitted by using two theoretical profiles with different effective temperatures, one for the core and other for the wings. Faraggiana & Bonifacio (1999) pointed out that this duplicity can be explained in terms of a binary system although some of

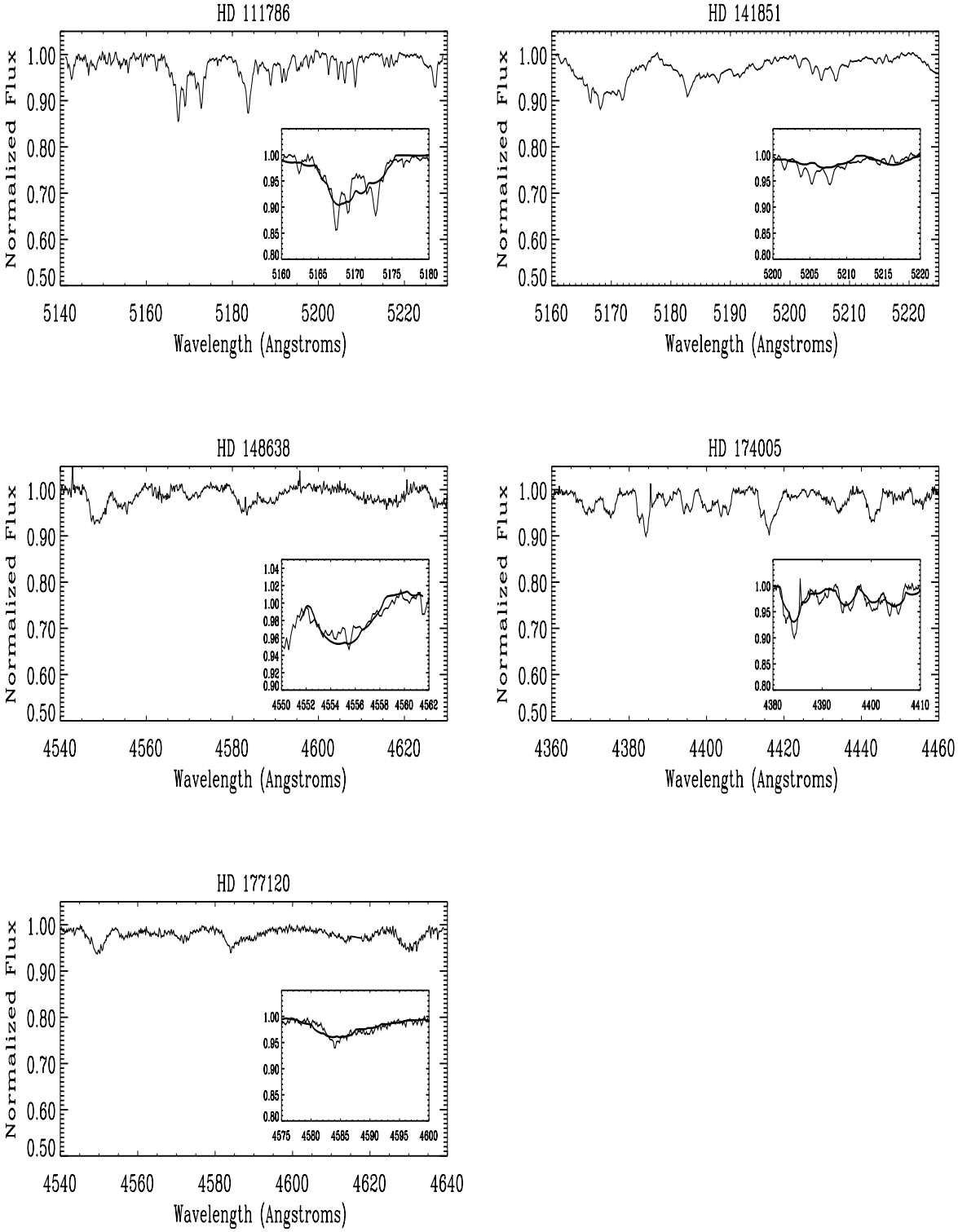

Fig. 1. Observed stars with composite spectra.

the stars catalogued as PHL objects (e.g., HD 142703, HD 142994, HD 204041) do not show in their spectra any sign of the presence of companion. Moreover, this scenario would not explain why PHL profiles are more frequent at lower temperatures as proposed by Iliev & Barzova (1993).

To ensure the reliability of the temperatures calculated using Balmer lines, they have been compared with those calculated using the photometric calibration by Moon & Dworetsky (1985) finding no systematic differences (Table 2).

Table 3. Stars with surface gravities derived from Hipparcos parallaxes. Ages have been derived using Main Sequence (Claret 1992) and Pre-Main Sequence (Palla 1993) evolutionary tracks.

Identification	Parallax	Bolometric Correction	$M_{\rm bol}$	log $(L/L_\odot)$	log $(M/M_\odot)$	log t	
						PMS	MS
HD 68758	6.80 ± 0.62	-0.32	0.37	1.74	0.38	6.21	8.63
HD 75654	12.82 ± 0.58	-0.15	1.77	1.18	0.27	6.92	8.97
HD 107233	12.32 ± 0.81	-0.17	2.65	0.82	0.20	7.17	8.93
HD 111005	5.75 ± 1.01	-0.15	1.62	1.23	0.28	6.84	8.61
HD 142703	18.89 ± 0.78	-0.25	2.26	0.98	0.22	7.00	9.13
HD 156954	12.18 ± 0.94	-0.09	3.03	0.67	0.17	7.30	8.50
HD 168740	14.03 ± 0.69	-0.20	1.66	1.22	0.23	6.90	9.32
HD 204041	11.46 ± 0.99	-0.32	1.43	1.31	0.29	6.90	8.91
HD 210111	12.70 ± 0.89	-0.25	1.65	1.22	0.28	6.80	8.31

5. Surface gravities

The method of calculating spectroscopic gravities using the standard technique of making abundances of both neutral and ionized iron lines agree was not used here due to the scarcity of usable Fe II lines in the observed wavelength range. Alternatively, surface gravities were derived for those stars with accurate parallaxes in the HIPPARCOS catalogue following a method similar to that described in Nissen et al. (1997). In short, the method relies on the basic relations

$$M_{\rm bol} = m_{\rm v} + 5 \log \pi + 5 + {\rm BC} \quad (1)$$

$$L = L_\odot \times 10^{0.4(M_{\rm bol,\odot} - M_{\rm bol})} \quad (2)$$

where $M_{\rm bol}$ is the bolometric absolute magnitude, $m_{\rm v}$ is the apparent visual magnitude, π is the trigonometrical parallax determined by HIPPARCOS (in arcseconds), BC is the bolometric correction and L is the luminosity. $L_\odot$ and $M_{\rm bol,\odot}$ refer to the solar luminosity and absolute bolometric magnitude, respectively. Visual magnitudes are from SIMBAD whereas the bolometric corrections were taken from Lang (1980). A value of $M_{\rm bol,\odot} = 4.71$ was adopted. Bolometric corrections from other authors (e.g. Bessell 1998) have been found to produce negligible differences in the derived quantities (luminosities and masses). Only stars with relative errors in parallax less than about 10% were considered to neglect bias in the estimation of the absolute magnitude (Brown et al. 1997).

The mass of the stars were calculated from its position in the log L–log $T_{\rm eff}$ diagram by interpolating in the isochrones given in Claret (1995). The mass so calculated was used as input value in the log $T_{\rm eff}$–log g diagram to obtain the surface gravity. A chemical composition $X = 0.70$, $Z = 0.02$ (solar abundance) was adopted. This is based on the fact that the main contribution to the overall metallicity is due to C, N, O (solar abundant in λ Bootis stars). Furthermore, there are strong indications that the λ Bootis phenomenon is restricted to the stellar surface (Holweger & Rentzsch-Holm 1995). The mixing length and core overshooting parameters were fixed to 1.52 and 2.0 respectively. Surfaces gravities are given in Table 2. Parallaxes, bolometric corrections, magnitudes, luminosities, masses and ages are displayed in Table 3. Age estimations for the sample stars indicate that they cover an area slightly above the Main Sequence. Surface gravities calculated using HIPPARCOS are only slightly higher than those derived using Moon & Dworetsky (1985) (HIPP $-$ MD85 $= 0.07 \pm 0.14$). A conservative value of Δ log $g = 0.15$ dex has been estimated based on errors in the bolometric correction and in the calculated mass.

6. Chemical analysis

The abundance analysis was performed making use of a modified version of the ATLAS9 code (Kurucz 1993) in which the classical mixing length theory used for the treatment of convection has been replaced by the turbulent theory implemented by Kupka (1999) as described in Sect. 4.

Since the wavelength coverage of our spectra is quite extensive, we have been restrictive in the selection of lines for abundance analysis. Weak lines with large errors in equivalent width due to noise and strong lines with a high sensitivity to errors in microturbulence were discarded. Moreover, the typically high rotational velocities of the λ Bootis stars produce a strong blending of the spectral lines and it is an additional limiting factor in the line selection. Only blended features formed by lines of the same element and ionization stage were considered (Fig. 2).

The abundance of the different elements were computed line by line by linearly interpolating in the grid of metallicity values for a given $T_{\rm eff}$ and log g, the final abundance being the average value. Results are displayed in Table 4 and plotted in form of abundance patterns in Fig. 3. For those program stars in common with Stürenburg (1993), abundances have been also displayed, showing good agreement.

Microturbulence was calculated in an independent way for each individual spectrum by making abundance results of weak and strong lines agree. We have used the iron lines since they are the most numerous and are spread over a wide range in equivalent width. In those cases where the

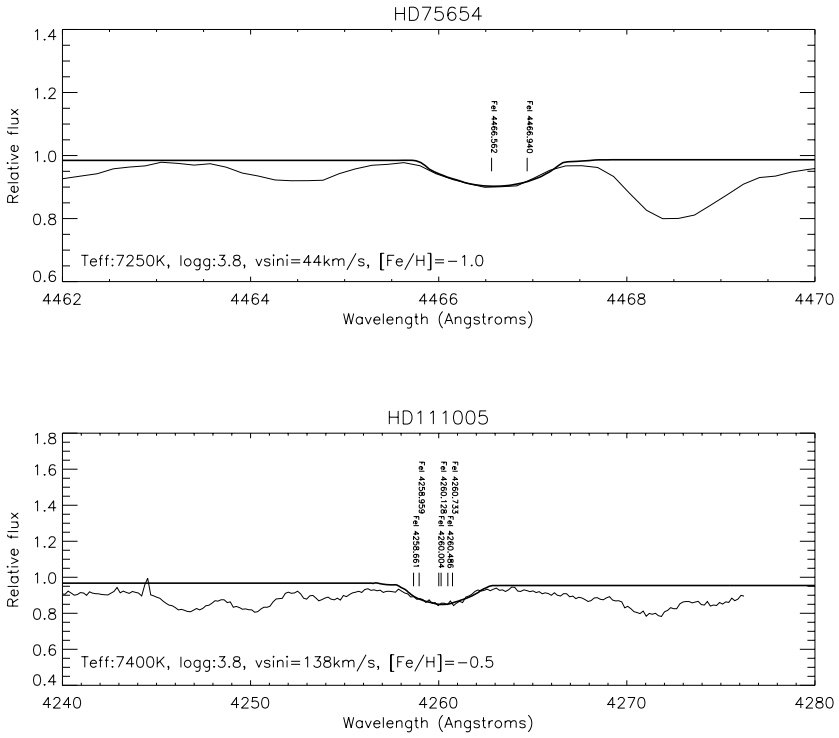

Fig. 2. Comparison between observed and synthetic spectra for two stars of our sample.

scarcity of Fe I lines prevents from using this method, a value of $\xi = 3.0$ kms^{-1} was adopted (Stürenburg 1993).

6.1. Estimated uncertainties

One source of uncertainty is the quality of the oscillator strengths values. To avoid using lines with log gf values of poor quality, a careful selection has been made using the most recent papers in the literature and the VALD database (Kupka et al. 1999). An average value was adopted. As a further test we compared, for every spectrum, the abundance value derived from every single line with the average value. Lines with abundance values clearly discrepant (which could be attributed to a wrong log gf) were discarded.

Another source of uncertainty results from the errors of the input atmospheric parameters. To get an estimation of how sensitive our results are to these errors we have derived the abundances of a synthetic spectrum with $T_{\rm eff}$: 7500 K, log g: 4.0, [M/H]: −1.0 varied by $\Delta T_{\rm eff} = \pm 200$ K, Δ log $g = \pm 0.3$ dex. Errors in metallicity of Δ[M/H] = 0.2 dex are obtained on average. As expected, the abundance of ions changes with changes in log g whereas the neutral species tend to have negligible changes. On the contrary, changes in $T_{\rm eff}$produce changes in the abundances derived from neutral species while the abundances derived from ions remain unchanged.

Uncertainties in the abundance values due to NLTE effects should also be included. However, according to Heiter et al. (1998), corrections due to non-LTE effects are of the same order as the abundance error bars in the range of temperature of our program stars making the LTE approach perfectly valid.

Finally, it must be stressed that some abundances rely in only one or few spectral lines so that the uncertainty is high.

7. Discussion

In order to search for correlations providing clues about the nature of λ Bootis stars, the abundances for our program stars have been compared with those of Procyon, a primary standard with solar metallicity (Steffen 1985). Chemical abundances of the class prototype, λ Boo, were taken from the literature (Paunzen et al. 1999b). As can be deduced from Table 4, all the program stars but one (HD 184190) show a clear metal deficiency when compared to Procyon. Moreover, it is quite evident that the candidate λ Bootis stars here analyzed do not resemble the abundance pattern of the class prototype, in particular for some chemical species (magnesium, titanium and iron). This result poses some concern with the idea of that λ Bootis stars form a well separate, chemically homogeneous group of the stars. On the contrary, this result reinforces the hypothesis proposed by Stürenburg (1993) that λ Bootis stars cover a continuous sequence of underabundances from very metal week to solar metallicities.

At this point, it would be necessary to reopen the question of the λ Bootis class definition. If the definition by Baschek & Searle (1969) – "... λ Bootis stars can be defined as stars whose composition resembles that of λ Boo itself" – is strictly adopted, then all the stars in our sample should be rejected as potential candidates to the

Table 4. Abundances of the program stars. In brackets is the number of spectra and the lines per spectrum used.

Identification	$v_{\rm mic}$	[MgI/H]	[CaI/H]	[ScII/H]	[TiII/H]	[MnI/H]
		[CrI/H]	[CrII/H]	[FeI/H]	[FeII/H]	
Procyon	2.0	0.21 ± 0.03 (2/2)	-0.19 ± 0.45 (4/1)	-0.02 (1/1)	0.17 ± 0.07 (4/3)	-0.03 (1/1)
		-0.05 ± 0.08 (3/2)	-0.08 ± 0.14 (2/1)	-0.18 ± 0.11 (4/14)	-0.07 ± 0.09 (4/1)	
HD 68758	3.0					
				-0.58 (1/1)		
HD 75654	3.5	-0.52 ± 0.18 (1/2)	-0.75 ± 0.08 (1/2)		-1.01 ± 0.29 (2/2)	-1.0 ± 0.42 (2/1)
		-1.13 ± 0.23 (1/2)	-1.07 (1/1)	-1.04 ± 0.14 (2/14)	-1.12 ± 0.13 (2/1)	
HD 81290	3.0	-1.07 ± 0.08 (2/2)	-0.89 (1/1)	-0.88 (1/1)	-1.10 ± 0.17 (4/2)	-0.73 ± 0.23 (2/1)
			-1.21 (1/1)	-1.22 ± 0.12 (4/12)	-0.93 ± 0.22 (3/1)	
HD 83041	3.0	-1.40 ± 0.17 (3/1)	-1.31 (1/1)	-0.86 (1/1)	-1.24 ± 0.16 (6/1)	
				-1.14 ± 0.11 (6/5)	-1.33 (1/1)	
HD 107233	4.0				-1.15 ± 0.15 (2/2)	
			-0.96 (1/1)		-1.14 ± 0.21 (2/8)	-1.13 ± 0.14 (2/1)
HD 109738	3.0					
				-0.83 ± 0.32 (2/2)	-1.25 (1/1)	
HD 111005	3.0				-0.13 ± 0.12 (3/2)	
				-0.39 ± 0.09 (4/5)	-0.33 ± 0.15 (3/1)	
HD 142703	3.0	-0.76 ± 0.06 (1/2)			-1.13 ± 0.1 (1/2)	
				-1.10 ± 0.12 (2/4)	-1.17 ± 0.08 (2/1)	
HD 142994	3.0					
				-0.56 ± 0.19 (4/1)		
HD 156954	2.5		-0.56 ± 0.07 (2/2)		-0.26 ± 0.10 (3/2)	
			-0.76 (1/1)	-0.75 ± 0.10 (3/11)	-0.57 ± 0.12 (3/1)	
HD 168740	3.0				-0.70 ± 0.08 (2/2)	
				-0.84 ± 0.06 (2/4)	-0.73 (1/1)	
HD 184190	3.0	0.20 (1/1)	-0.18 (1/1)		0.55 ± 0.12 (1/2)	
		0.39 ± 0.05 (1/3)	0.0 (1/1)	0.17 ± 0.19 (1/16)		
HD 193281	4.0	-0.11 ± 0.07 (2/2)			-0.61 ± 0.09 (3/2)	
				-1.13 ± 0.07 (3/3)	-0.84 ± 0.03 (2/1)	
HD 204041	3.0	-1.06 ± 0.09 (1/2)			-1.47 ± 0.1 (3/2)	
			-1.08 (1/1)	$-1.00 \pm .130$ (3/6)	-0.80 ± 0.13 (3/1)	
HD 210111	3.0	-0.98 ± 0.12 (1/2)	-0.85 ± 0.12 (1/2)		-1.10 ± 0.06 (3/2)	
		-1.33 ± 0.10 (2/1)	-1.15 (1/1)	-0.88 ± 0.12 (3/9)	-0.82 ± 0.08 (3/1)	

λ Bootis group. On the contrary, if the more conservative definition given by Paunzen et al. (1997a) is considered – "... λ Bootis stars are Population I, metal-weak (except for C, N, O, S) stars" –, all the stars (except HD 184190) could be catalogued as members of the λ Bootis class provided that they show solar abundances for carbon, nitrogen, oxygen and sulphur. It is of fundamental importance to stress this point since the λ Bootis phenomenon is not ascribed to an overall metal deficiency but to a mechanism able to produce underabundances of the heavy elements contrasting with the solar abundances of C, N, O and S. None of these species have been analyzed in this paper due to the lack of spectral lines fulfilling the requirements quoted in Sect. 6. NLTE abundances of nitrogen and sulphur for the program stars will be part of a subsequent paper (Kamp et al. 2001).

The observed distribution of the abundance values does not permit us to discriminate between the theories proposed to explain the λ Bootis phenomenon. It could be explained in terms of the diffusion/mass-loss hypothesis on the basis of different stages of the diffusion process. Under the assumption of the accretion hypothesis, the observed differential deficiencies would reflect different scenarios in the gas-dust decoupling ascribed to different disk properties. Moreover, the binarity theories would be also supported.

The relation between metallicity and $v \sin i$, $\log g$, $T_{\rm eff}$ has been plotted in Fig. 4. Whereas no obvious

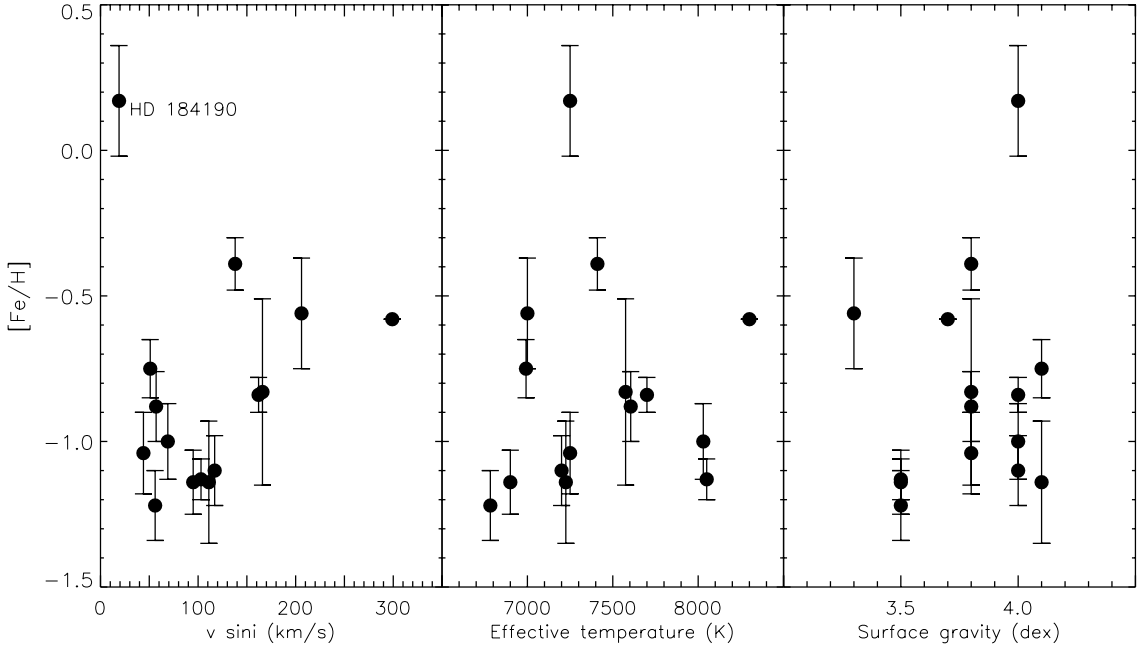

Fig. 4. Relation between physical parameters.

correlation between log g and $T_{\rm eff}$ with [Fe/H] exists, there is evidence for a connection between projected rotational velocities and metallicity in the sense that the metallicity is higher when $v \sin i$ increases, although the correlation coefficient ($\rho = 0.59$) and the small number of measurements ($n = 14$) do not permit to obtain any statistically significant conclusion. A similar result was found by Holweger & Rentzsch-Holm (1995) using calcium abundances derived from the Ca II K line. If, after the determination of the C, N, O and S abundances the membership of the program stars to the λ Bootis group is finally confirmed, this result would nicely fit with the accretion theory: for large $v \sin i$ the meridional circulation mixes material of solar composition from the stellar interior into the convection zone so that any surface contamination due accretion of circumstellar material should vanish.

8. Conclusions

Physical parameters for a sample of suspected λ Bootis stars have been obtained. Effective temperatures were determined both photometrically and spectroscopically to identify potential problems affecting the methods (peculiar Balmer line profiles, presence of circumstellar gas and dust, ...), the values so obtained showing an excellent agreement. The chemical analysis shows a wide range of underabundances for the different studied elements suggesting a continuous distribution from very metal-weak to solar metallicities. One of the stars, HD 184190, does not fit the overall distribution and it can be excluded from the λ Bootis group. The abundance distribution does not permit us to shed light on the conflict of the theories on the λ Bootis nature, although the relation found between projected rotational velocities and iron abundances seems to agree well with the accretion hypothesis. Accurate C, N, O, S abundances for the program stars are required to confirm their membership to the λ Bootis group and this will be partly covered (N, S abundances) by a subsequent paper (Kamp et al. 2001).

Acknowledgements. The authors acknowledge use of the CCD and data acquisition system supported under U.S. National Science Foundation grant AST-90-15827 to R. M. Rich.

References

Abt, H. A. 1985, ApJS, 59, 95
Andrievsky, S. M. 1997, A&A, 321, 838
Andrievsky, S. M., & Paunzen, E. 2000, MNRAS, 313, 547
Baschek, B., & Searle, L. 1969, ApJ, 155, 537
Bessel, M. S., Castelli, F., & Plez, B. 1998, A&A, 333, 231
Bohlender, D. A., Gonzalez, J. F., & Matthews, J. M. 1999, A&A, 350, 553
Brown, A. G. A., Arenou, F., van Leeuven, F., Lindegren, L., & Luri, X. 1997, ESA-SP, 402, 63
Canuto, V. M., Goldman, I., & Mazzitelli, I. 1996, ApJ, 473, 550
Claret, A., & Giménez, A. 1992, A&AS, 96, 255
Claret, A. 1995, A&AS, 109, 441
Charbonneau, P. 1991, ApJ, 372, L33
Faraggiana, R., Gerbaldi, M., & Burnage, R. 1997, A&A, 318, L21
Faraggiana, R., & Bonifacio, P. 1999, A&A, 349, 521
Gardiner, R. B., Kupka, F., & Smalley, B. 1999, A&A, 347, 876
Gray, R. O. 1988, AJ, 95, 220
Gray, D. F. 1992, in The observation and analysis of stellar photospheres (Cambridge Univ. Press), 368
Gray, R. O., & Corbally, C. J. 1988, AJ, 116, 2530
Gray, R. O., & Corbally, C. J. 1993, ApJ, 106, 632

Griffin, R., & Griffin, R. 1979, in A photospheric atlas of the spectrum of Procyon λλ3140–7470 Å (The Observatory, Cambridge)
Heiter, U., Kupka, F., Paunzen, E., Weiss, W. W., & Gelbmann, M. 1998, A&A, 335, 1009
Holweger, H., Hempel, M., & Kamp, I. 1999, A&A, 350, 603
Holweger, H., & Rentzsch-Holm, I. 1995, A&A, 303, 819
Iliev, I. K., & Barzova, I. S. 1993, ApSS, 208, 277
Iliev, I. K., & Barzova, I. S. 1995, A&A, 302, 735
Kamp, I., Iliev, I., Paunzen, E., et al. 2001, submitted
King, J. R. 1994, MNRAS, 269, 209
Kupka, F. 1999, priv. comm.
Kupka, F., Piskunov, N. E., Ryabchikova, T. A., Stempels, H. C., & Weiss, W. W. 1999, A&AS, 138, 119
Kurucz, R. L. 1993, CD-ROM 1-23, Smithsonian Astrophysical Observatory
Lang, K. R., in Astrophysical Formulae (Springer-Verlag), 564
Michaud, G., & Charland, Y. 1986, ApJ, 311, 326
Moon, T. T., & Dworetsky, M. M. 1985, MNRAS, 217, 305
Moore, C. E., Minnaer, M. G. J., & Houtgast, J. 1966, in National Bureau of Standards, The Solar Spectrum 2935 Å to 8770 Å
Nissen, P. E., Høg, E., & Schuster, W. J. 1997, ESA-SP, 402, 657
North, P., Berthet, S., & Lanz, T. 1994, A&A, 281, 775
Palla, F., & Stahler, S. W. 1993, ApJ, 418, 414
Paunzen, E. 1997, A&A, 326, L29
Paunzen, E. 2000, Ph.D. Thesis, Univ. of Vienna, Austria
Paunzen, E., & Gray, R. O. 1997, A&AS, 126, 407
Paunzen, E., Weiss, W. W., Heiter, U., & North, P. 1997, A&AS, 123, 93
Paunzen, E., Weiss, W. W., Martinez, P., et al. 1998a, A&A, 330, 605
Paunzen, E., Weiss, W. W., Kuschnig, R., et al. 1998b, A&A, 335, 533
Paunzen, E., Kamp, I., Iliev, I. K., et al. 1999a, A&A, 345, 597
Paunzen, E., Andrievsky, S. M., Chernyshova, I. V., et al. 1999b, A&A, 351, 981
Smalley, B., & Kupka, F. 1997, A&A, 328, 349
Solano, E., & Fernley, J. 1997, A&AS, 122, 131
Solano, E., & Paunzen, E. 1998, A&A, 331, 633
Solano, E., & Paunzen, E. 1999, A&A, 348, 825
Steffen, M. 1985, A&A, 59, 403
Stürenburg, S. 1993, A&A, 277, 139
Turcotte, S., & Charbonneau, P. 1993, ApJ, 413, 376
Venn, K. A., & Lambert, D. L. 1990, ApJ, 363, 234
Waters, L. B. F. M., Trams, N. R., & Waelkens, C. 1992, A&A, 262, L37